Robust Signal Quality Monitoring and Detection of Evil Waveforms

R. Eric Phelts, Dennis M. Akos, Per Enge
Department of Aeronautics and Astronautics, Stanford University

BIOGRAPHY

R. Eric Phelts is a Ph.D. candidate in the Department of Aeronautics and Astronautics at Stanford University. He received his B.S. in Mechanical Engineering from Georgia Institute of Technology in 1995, and his M.S. in Mechanical Engineering from Stanford University in 1997. His research involves multipath mitigation techniques and satellite signal anomalies.

Dennis M. Akos completed the Ph.D. degree in Electrical Engineering at Ohio University conducting his graduate research within the Avionics Engineering Center. After completing his graduation he has served as a faculty member with Luleå Technical University, Sweden and is currently a research associate with the GPS Laboratory at Stanford University. His research interests include GPS/CDMA receiver architectures, RF design, and software radios.

Per Enge is an Associate Professor of Aeronautics and Astronautics at Stanford University, where he has been on the faculty since 1992. His research deals with differential operation of GPS for landing aircraft. Previously, he was an Associate Professor of Electrical Engineering at Worchester Polytechnic Institute.

ABSTRACT

The ability to monitor and detect problematic distortions in the received GPS-SPS signal is a task of critical importance. Detection of these satellite signal anomalies or "evil waveforms" can be accomplished using detailed monitoring of the correlation peak. Using the "Second-Order Step" threat model for evil waveforms, previous analysis has attempted to show that monitoring sufficient to satisfy GBAS and SBAS requirements for Category I precision approaches may be obtained from a receiver design that requires minimal modifications to existing GPS hardware. A "robust" signal quality monitor (SQM) design methodology has been developed for this purpose.

This report evaluates the best current evil waveform (EWF) signal quality monitoring configuration, SQM2b, using this methodology. First, it compares the maximum regional pseudorange errors (PRE's), computed at varying elevation angles, to the maximum allowable pseudorange (MERR) errors. Second, it examines the sensitivity of these results to differential group delay variations of up to 150ns. In addition, it examines the effects of user filter magnitude response.

Using SQM2b, neither group delay variations nor changing MERR's were found to pose a threat to standard E-L correlators in any of the four protected regions. However, they did induce some small, unacceptable $\Delta\Delta$ receiver errors. To account for this, a "notch" was removed from the critical protected region to exclude those unprotectable $\Delta\Delta$ receiver configurations. It was also shown that user PRE's were sensitive to transition bandwidth variations. To mitigate this sensitivity it was recommended that the minimum airborne filter transition bandwidth be upper-bounded by that of the 6^{th}-order Butterworth filter.

BACKGROUND

Satellite signal anomalies, or "evil waveforms" (EWF's), result from a failure of the signal generating hardware on one of the GPS space vehicles (SV). These anomalies may cause severe distortions of the autocorrelation peak inside GPS receivers. In local area differential systems, undetected evil waveforms may result in large pseudorange errors, which in general do not cancel. One such failure occurred on SV19 in October of 1993. It caused differential pseudorange errors on the order of 3 to 8 meters [1].

The Local Area Augmentation System (LAAS) requires that a monitoring system be placed at ground

reference stations to detect these failures when they occur. The envisioned signal quality monitoring (SQM) scheme would consist of one or more (wideband) GPS receivers having several correlators configured to sample the correlation peak at multiple locations in order to determine its level of distortion. Rather than simply sending corrupted differential corrections to airborne users, if an EWF is detected the SV would then be flagged and its pseudorange subsequently removed from the users position solution.

For designing an SQM configuration, the "second-order step" model was developed [1]. This model assumes the anomalous waveform is some combination of second-order ringing (an analog failure mode) and lead/lag (a digital failure mode) of the pseudorandom noise (PRN) code chips. Threat Models (TM) A, B, and C are used to characterize these failure modes. (See Figures 1,2,3). The model parameter bounds for f_d (damped natural frequency) σ, (damping) and Δ (lead/lag) are provided in Figure 4. An effective ground monitoring implementation would detect any and all EWF's that would result in unacceptably large differential PRE's.

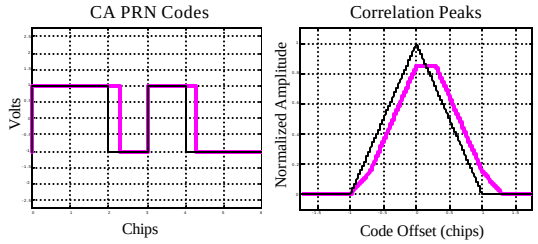

Figure 1. Threat Model A: digital failure mode

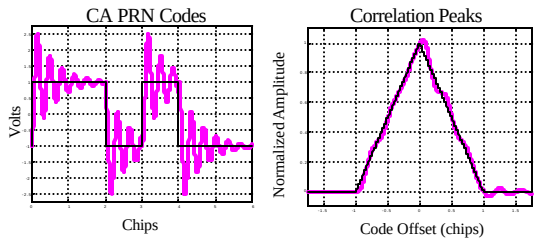

Figure 2. Threat Model B: Analog failure mode

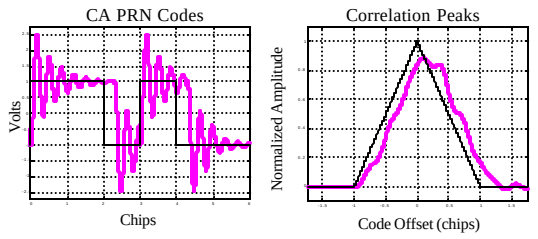

Figure 3. Threat Model C: Combination (analog and digital failure modes)

The SQM performs symmetry tests on the received correlation peak. However, the detection capability of a particular SQM is limited by the nominal distortion of the correlation peak. This distortion is quantified in terms of (test-specific) minimum detectable errors (MDE's). The MDE's are dependent on elevation angle and dominated by multipath conditions at a particular site [2].

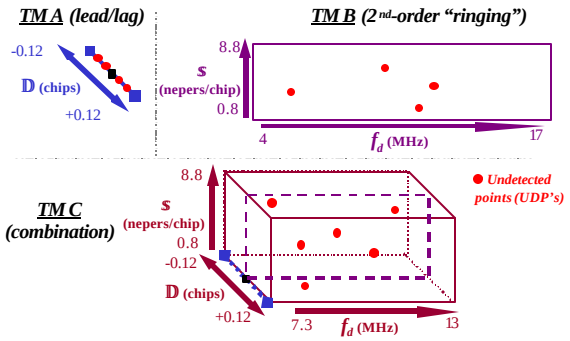

Figure 4. EWF parameter threat space

Once valid MDE's are obtained, SQM designs may be modeled and evaluated in simulation. An illustration of the simulation process is shown in Figure 5. If any EWF's are undetectable by a particular SQM configuration, it is necessary to determine their impact on the differential pseudorange errors (PRE's) of airborne users. These users may have vastly different receiver configurations since receiver manufacturers desire the freedom to implement both narrow and wide precorrelation bandwidths (PCB's) with narrow and/or wide correlator spacings. (See Figure 6.)

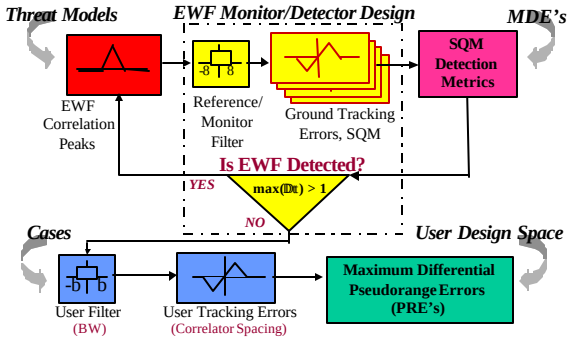

Figure 5. SQM simulation and evaluation process.

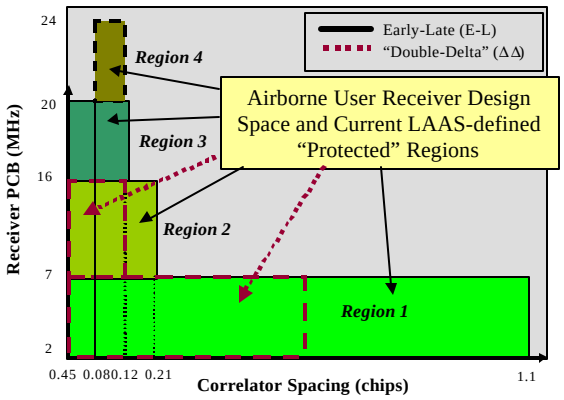

Figure 6. Airborne user receiver configuration (design) space.

An effective SQM design would keep the maximum differential PRE's for these users below the maximum allowable error (MERR) corresponding to that elevation angle [3,4]. (A sample result of this simulation and evaluation process is shown in Figures 7 and 8.) The implemented SQM should also be robust to variations in user filter group delays and magnitude responses.

For LAAS, the current goal (for Category I Precision Approach) is to protect the L-shaped region of this two-dimensional user design space using a practical ground SQM scheme. Previous research and analysis has converged on such an SQM implementation: SQM2b [2,5,6,7]. This paper describes the methodology used for validating SQM2b as a robust signal quality monitor for CAT 1 LAAS.

Max PRE's: Analog Failure Mode (7.3MHz<f_d<17MHz)

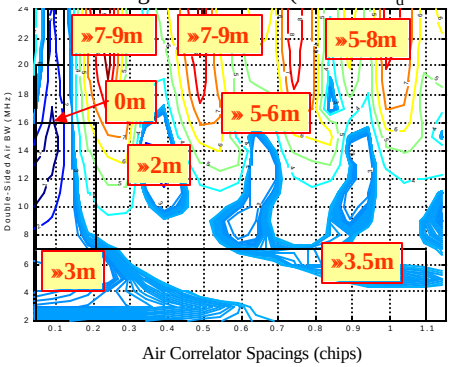

Figure 7. Sample "contour plot" of maximum PRE's for a subset of TM B (full range of s used; *no SQM*).

Max PRE's: Analog Failure Mode (7.3MHz<f_d<17MHz)

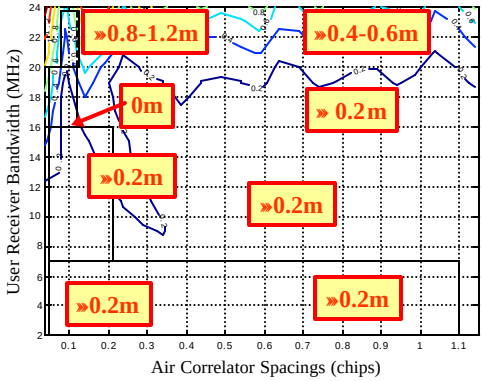

Figure 8. Sample "contour plot" of maximum PRE's for a subset of TM B (full range of s used; *with SQM2b*).

Minimum Detectable Errors (MDE's)

Figure 9 below shows the correlator spacing configuration for SQM2b. It consists of 3 correlator pairs with Early-Late spacings of 0.1, 0.15, and 0.2 chips. From these spacings a total of 11 symmetry tests may be formed: 9 "Ratio Tests" and 2 "Delta Tests." These tests are described in more detail in [2,5,7]. Each of these tests required a corresponding set of elevation angle-dependant MDE's.

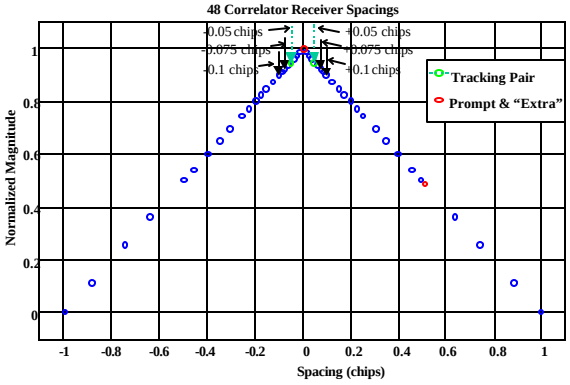

Figure 9. Actual correlator configuration (spacing/locations) for SQM2b.

Minimum Detectable Error (MDE) data was taken at Stanford University. Correlation peak measurements were taken for live satellite passes and were grouped into bins according to elevation angles [2,5]. The MDE's used for a given elevation angle were assumed to correspond to the mean elevation angle of each of the 5-degree bins from 2.5 to 87.5 degrees. Third-order polynomials were fit to the measured data. These relations were subsequently used to compute valid MDE's for arbitrary elevation angles

between 5 and 90 degrees. The fit results are summarized in the tables below.

Note that a curve-fit approach was employed (as opposed to a discrete elevation angle "binning" approach) in attempt to reduce the influence of uncharacteristic deviations caused by siting effects. The curve-fit applies to elevation angles that may not be well characterized by a particular bin. The discrete-bin approach may require overly conservative MDE's and/or MERR's to properly validate the SQM.

Fit Results:

$$MDE = a_3\theta^3 + a_2\theta^2 + a_1\theta + a_0,$$

where

θ = Elevation angle in degrees

a_0, a_1, a_2, a_3 = 3rd –order polynomial coefficients

D-Test:

	a_3	a_2	a_1	a_0
$\mathbf{D}_{\pm 0.075, \pm 0.05}$	-5.5345e-009	1.6638e-006	-1.6604e-004	6.3401e-003
$\mathbf{D}_{\pm 0.1, \pm 0.05}$	-1.5115e-008	4.0539e-006	-3.7768e-004	1.3769e-002

Average Ratio Tests:

	a_3	a_2	a_1	a_0
$\mathbf{R}_{\pm 0.05av,P}$	-1.5836e-008	3.6739e-006	-2.8795e-004	9.3079e-003
$\mathbf{R}_{\pm 0.075av,P}$	-3.2462e-008	7.0746e-006	-5.2628e-004	1.6099e-002
$\mathbf{R}_{\pm 0.1av,P}$	1.6099e-002	8.0973e-006	-6.3291e-004	2.0298e-002

Negative Ratio Tests:

	a_3	a_2	a_1	a_0
$\mathbf{R}_{-0.05,P}$	-9.9465e-009	2.7144e-006	-2.4363e-004	8.8196e-003
$\mathbf{R}_{-0.075,P}$	-2.0817e-008	4.5971e-006	-3.4226e-004	1.0587e-002
$\mathbf{R}_{-0.1,P}$	-1.2278e-008	3.1656e-006	-2.6544e-004	9.0253e-003

Positive Ratio Test Results:

	a_3	a_2	a_1	a_0
$\mathbf{R}_{+0.05,P}$	-1.8875e-008	4.2323e-006	-3.2149e-004	1.0079e-002
$\mathbf{R}_{+0.075,P}$	-4.0849e-008	9.1818e-006	-7.1191e-004	2.2598e-002
$\mathbf{R}_{+0.1,P}$	-5.4957e-008	1.2696e-005	-1.0296e-003	3.4024e-002

Maximum Allowable Error (MERR) Analysis

The MERR curves can be obtained as a function of elevation angle from the σ_{lgf} equations in [4] for both 2 and 3-monitor receiver cases. The multipath at each of the 2 or 3 different antenna locations (one for each respective monitor receiver) is assumed to be independent. Accordingly, the MDE's may be reduced by the square root of 2 or 3 for these cases, respectively.

Procedure

SQM2b was implemented as the ground monitoring correlator spacing configuration. Whenever possible conservatively-inflated (120% of the curve-fit) (SU) MDE's were used. MERR's for the 2 and 3 monitor receiver cases were compared against the respective resulting contour plots generated for each elevation angle.

The SQM2b MERR investigation proceeded as follows:

1) Using the lowest elevation angle MDE's, compute the maximum user PRE's (i.e., airborne receiver contour plots) for a given threat model.
2) Compare maximum contour within any of the 4 (E-L and $\Delta\Delta$) protected regions to the MERR corresponding to that elevation angle.
3) Repeat procedure until maximum PRE within protected regions is below the minimum MERR (corresponding to a 90-degree elevation angle satellite) and/or until the elevation angle equals 90°.

An unacceptable condition exists if the maximum PRE ever exceeds the corresponding MERR for a particular elevation angle.

MERR Analysis Results

The results for Threat models A, B, and C, assuming both 2 and 3 monitor receivers, are given below (in Figures 10-16) for the standard E-L and the $\Delta\Delta$ correlator receivers, respectively. For Threat Model C, the $\Delta\Delta$ receivers were found to produce unacceptably high errors (for both the 2 and 3 monitor receiver cases) using 120% MDE's and even 100% MDE assumptions. Consequently, the $\Delta\Delta$ receiver (2 and 3 ground monitors, 100% MDE) cases were determined to be most critical and were subsequently singled out for more detailed analysis.

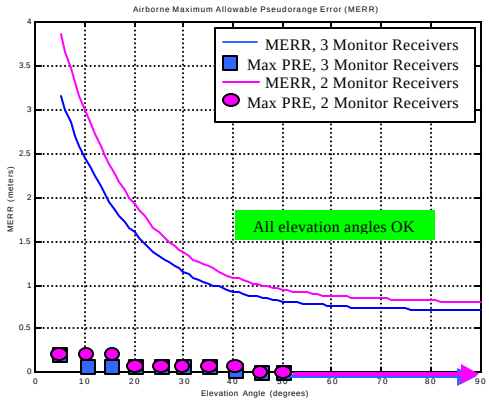

Figure 10. MERR Analysis – TM A (120% MDE's) – E-L Correlators (including Region 4)

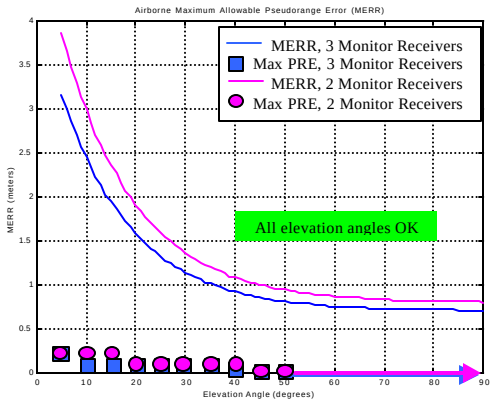

Figure 11. MERR Analysis – TM A (120% MDE's) – DD Correlators

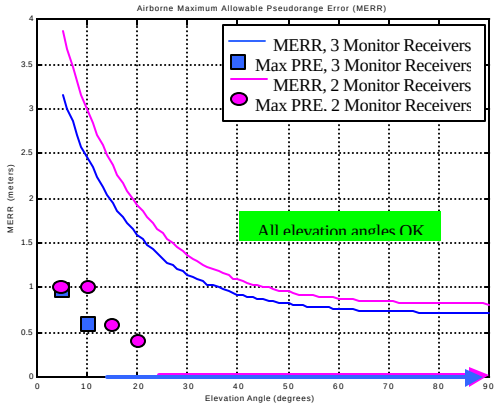

Figure 12. MERR Analysis – TM B (120% MDE's) – E-L Correlators (including Region 4)

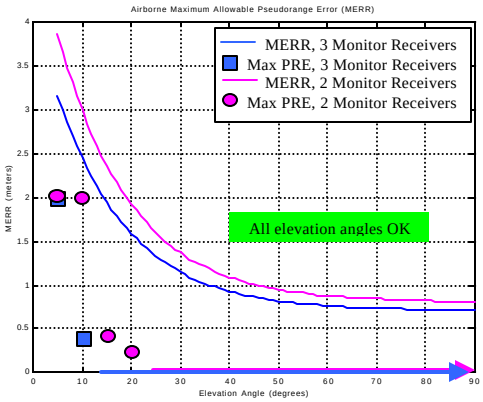

Figure 13. MERR Analysis – TM B (120% MDE's) – DD Correlators

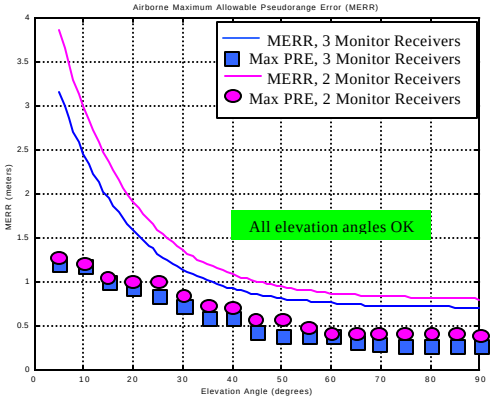

Figure 14. MERR Analysis – TM C (120% MDE's) – E-L Correlators (including Region 4)

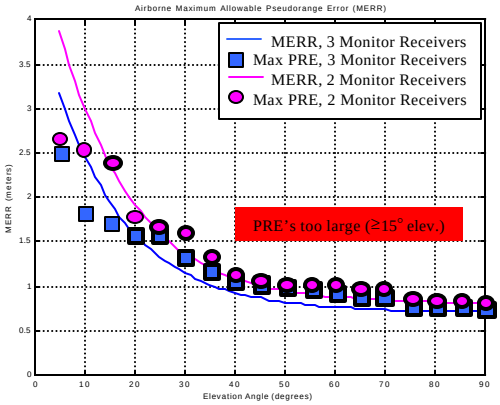

Figure 15. MERR Analysis – TM C (120% MDE's) – DD Correlators

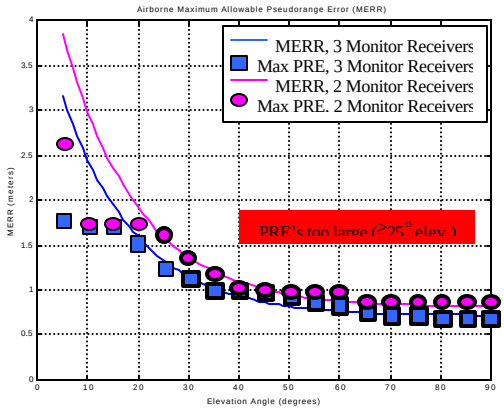

Figure 16. MERR Analysis – TM C (100% MDE's) – DD Correlators

Differential Group Delay Analysis

Methodology

To isolate the differential group delay (dT_{Gd}) parameter for a sensitivity analysis, for a given 3dB bandwidth the user filter magnitude response was constrained and the dT_{Gd} was varied from 0 to 150ns. A Butterworth filter design was selected as the baseline model (magnitude constraint) for the user filter implementations for the following reasons:

- They are simple to design and require relatively low orders for satisfactory implementations.
- Butterworth filters have minimal passband magnitude variations as a function of frequency.
- Most of the SQM analysis to date (by Stanford, STNA, and others) has employed a 6th-order Butterworth filter as the user filter (and on the ground). This analysis may assist in determining the generality of those results. [1,6]

In addition, a FIR (zero-dT_{Gd}) filter was implemented as the ground differential reference/monitor receiver (16MHz) filter to remove the effects of the reference/monitor receiver's dT_{Gd} from consideration.

Filter Design Procedure:

1) A stable digital Butterworth filter was designed to have a maximum dT_{Gd} of 150ns.
2) The group delay response of this filter was scaled to have a maximum dT_{Gd}'s of 30, 60, 90, 120, and 150ns respectively.
3) A new complex magnitude response was constructed using the magnitude of the original design and the new phase responses (the integrals of the scaled dT_{Gd}'s).
4) New stable transfer functions were obtained by finding the inverse frequency responses of the new complex magnitudes.
5) Filter magnitudes, phase and dT_{Gd}'s were plotted graphically to verify they were stable and all constraints were met. (See Figure 17.)

Note that the resulting filter magnitude responses were not all identical. In fact, the larger-group delay implementations were better described by the original (14th-order) IIR digital Butterworth designs. (As the dT_{Gd}'s approach zero, the filter becomes more appropriately described by a FIR design.) As a result, the magnitude responses are approximately equal for all implementations *except the 30ns dT_{Gd} design*. This means high-frequency EWF's (e.g., those with f_d's above the 3dB bandwidth) for that filter were attenuated significantly less than for the others. The dashed line depicts the characteristics of the 6th-order Butterworth filter for comparison.

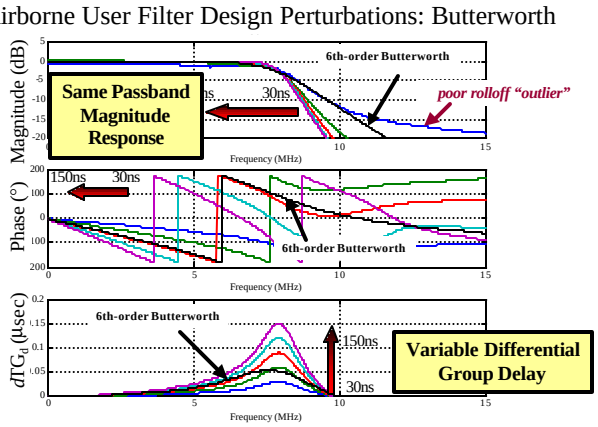

Figure 17. Butterworth filter designs with varying group delays.

Differential Group Delay Analysis Results

The MERR analysis revealed that the smallest margins (the highest PRE's) exist for only a few critical airborne receiver configurations. The figure below graphically illustrates four of these configurations (of the 3 primary Protected Regions) for which the group delay variations were explored. Note that two additional points—at 24MHz precorrelation bandwidth (PCB), $0.08T_c$ and $0.12T_c$, respectively—were also examined for the E-L receivers of Region 4 (using SQM2b only).

The next several figures plot the maximum user PRE's as a function of f_d. For each EWF frequency, f_d, the user (at a selected correlator spacing and PCB) PRE was computed. This error was maximized over all σ and Δ. A total of six curves are shown on each

plot. Each curve corresponds to a filter with a different group delay; the dT_{Gd}'s are indicated in the legend. A vertical (dotted) line was plotted to indicate the single-sided user receiver precorrelation (3dB) bandwidth; a horizontal (dashed) line indicates the MERR for the given elevation angle.

Group delay analyses were performed with and without implementing SQM. Without SQM, the results indicate PRE variations of only 1-2 meters. (See Figures 18-22.) With monitoring, the Threat Model C EWF's were tested at an elevation angle of 30° (a conservative angle by MERR analysis results). For the E-L receivers, the PRE sensitivity using SQM2b was generally <1m [8]. However, since the ΔΔ correlators in the 16MHz, 0.045Tc corner of Region 2 violated the MERR's (even for 100% MDE's), these configurations need to be excluded. (See Figure 22.) The group delay analysis results for this region are provided in the subsection entitled, "ΔΔ Correlators - Region 2 Notch Analysis."

No SQM: E-L Correlators

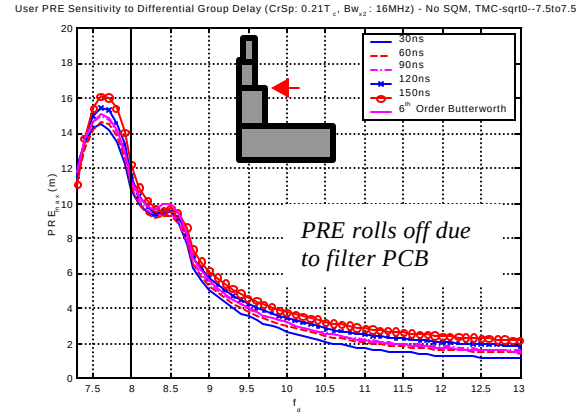

Figure 18. E-L correlator dT_{Gd}'s (16MHz, 0.21Tc; no SQM)

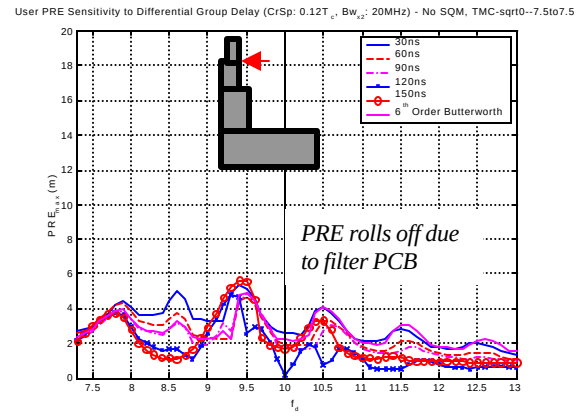

Figure 19. E-L correlator dT_{Gd}'s (20MHz, 0.12Tc; no SQM)

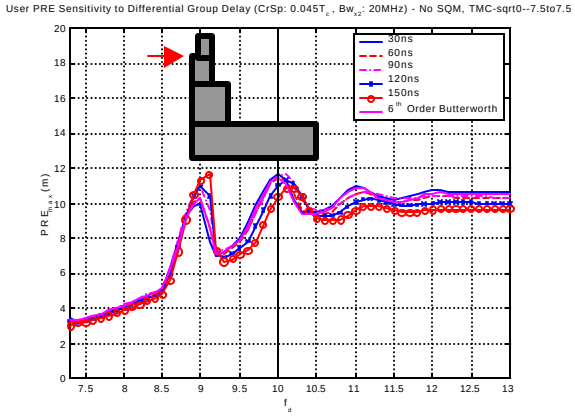

Figure 20. E-L correlator dT_{Gd}'s (20MHz, 0.045Tc; no SQM)

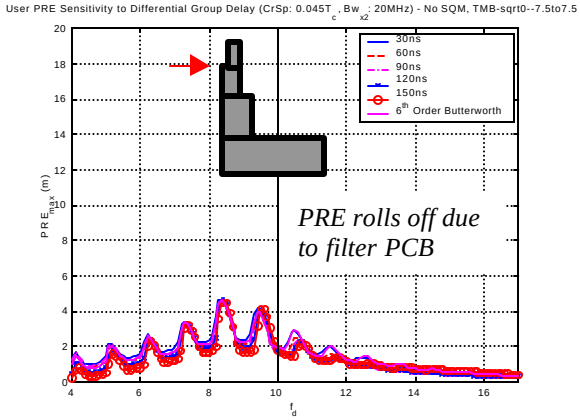

Figure 21. E-L correlator dT_{Gd}'s (20MHz, 0.045Tc; no SQM)

No SQM - ΔΔ Correlators

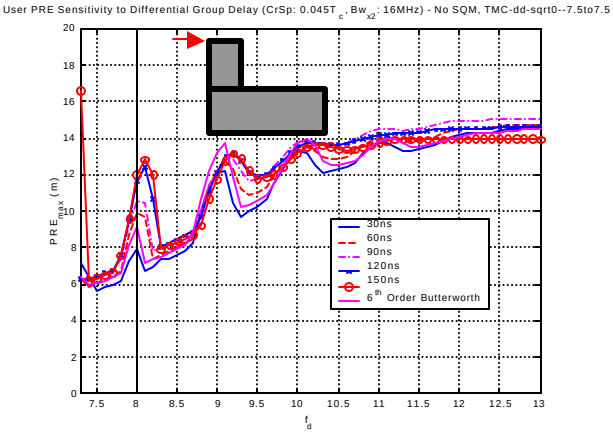

Figure 22. DD correlator dT_{Gd}'s (16MHz, 0.045Tc; no SQM)

Note that for this extremely narrow correlator spacing (and wide bandwidth) the maximum PRE's do not roll off as f_d increases. This is because the lead/lag

errors dominate. The flattening of the peak due to large Δ is not filtered by the user front-end bandwidth. The figure below illustrates that the PRE's for the same user receiver configuration do in fact roll off when Δ is removed (i.e., TM B).

ΔΔ Correlators - Region 2 Notch Analysis

From the previous MERR analysis, it became clear that users employing ΔΔ correlators cannot be adequately protected using SQM2b. The PRE's only exceed the MERR's, however, in a small area at the 0.045-chip and 16MHz corner of Region II of the ΔΔ space. A small rectangular section or "notch" can be removed from this region to exclude it from the allowable design space.

For elevation angles between 20 and 70 degrees, three corners of the rectangular notch were examined for acceptable PRE's in the presence of varying group delays. *Only a few select cases where the PRE's for the 6th-order Butterworth filter exceeded the MERR are shown here*. (See Figures 23-28.) Due to its extremely poor magnitude response, the 30ns curve exceeded the MERR for many elevation angles. (This condition is analyzed further in the section entitled "Magnitude Response Analysis".)

16.0MHz, 0.07T_c chip spacing -2 Monitor Receivers – 100% MDE's
(20°-70° elev.; 0 MERR crossings)

16.0MHz, 0.06T_c chip spacing -2 Monitor Receivers – 100% MDE's
(20°-70° elev.; 8 total MERR crossings, 2 shown below)

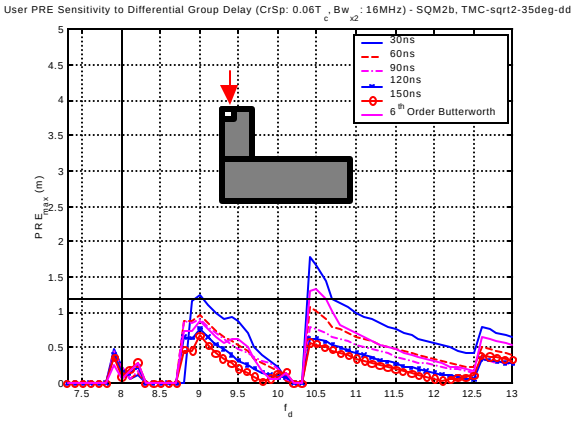

Figure 23. DD correlator dT_{Gd}'s using SQM2b (16.0MHz, 0.06T_c chip spacing; 2 Monitor Receivers, 100% MDE's; 35° elev.)

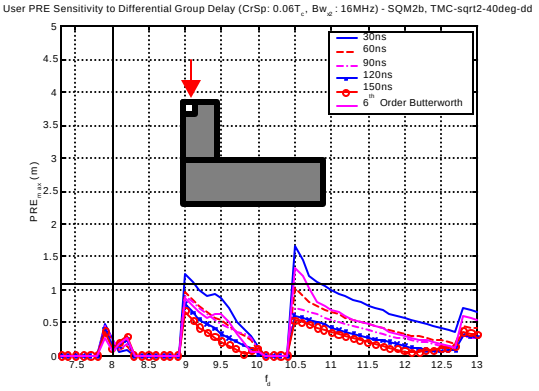

Figure 24. DD correlator dT_{Gd}'s using SQM2b (16.0MHz, 0.06T_c chip spacing; 2 Monitor Receivers, 100% MDE's; 40° elev.)

14.5MHz, 0.05T_c chip spacing -3 Monitor Receivers – 100% MDE's
(20°-70° elev.; 2 total MERR crossings)

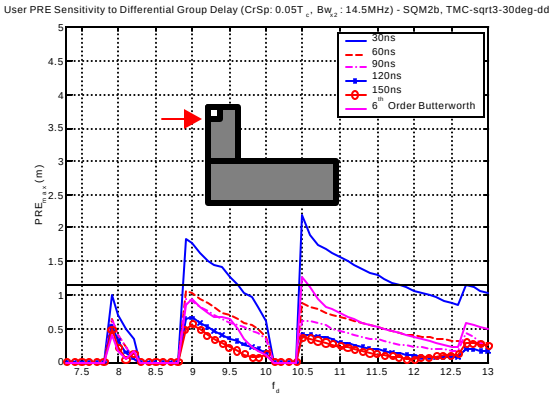

Figure 25. DD correlator dT_{Gd}'s using SQM2b (14.5MHz, 0.05T_c chip spacing; 3 Monitor Receivers, 100% MDE's; 30° elev.)

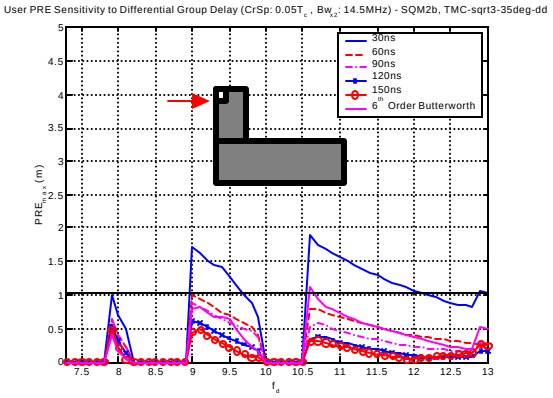

Figure 26. DD correlator dT_{Gd}'s using SQM2b (14.5MHz, 0.05T_c chip spacing; 3 Monitor Receivers, 100% MDE's; 45° elev.)

14.0MHz, 0.05T_c chip spacing -2 Monitor Receivers – 100% MDE's
(20°-70° elev.; 1 MERR crossing, <10cm)

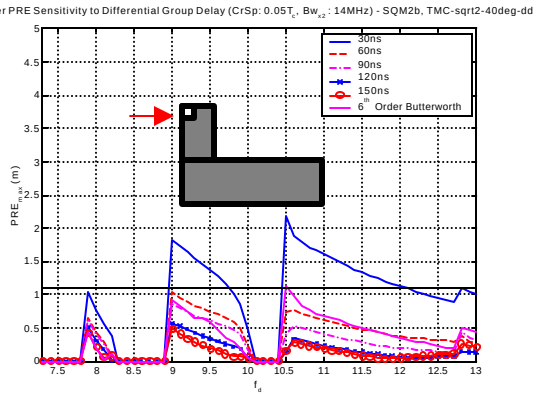

Figure 27. DD correlator dT_{Gd}'s using SQM2b (14.0MHz, 0.05T_c chip spacing; 2 Monitor Receivers, 100% MDE's; 40° elev.)

14.0MHz, 0.05T_c chip spacing - 3 Monitor Receivers – 100% MDE's
(20°-70° elev.; 0 MERR crossings)

To substantiate the assertion that the magnitude response (as opposed to small dT_{Gd}) causes the relatively poor performance of the 30ns filter, the same analysis was performed using an FIR (zero-dT_{Gd}) airborne filter. Only the result for the 14MHz, 0.05Tc ΔΔ case (100% MDE's) is shown (in Figure 28) below. If the PRE's were sensitive to small dT_{Gd}, the FIR curve would be significantly higher (i.e., worse) than the 6th-order Butterworth (and also the 30ns curve shown above). In fact the FIR performance here is much better than that of the 6th-order Butterworth. This is because the FIR filter used (300-tap Hamming window) has a much faster roll-off than the Butterworth. (See Figure 29.) Clearly, filter magnitude response in the transition band dominates the sensitivity of these curves [RR].

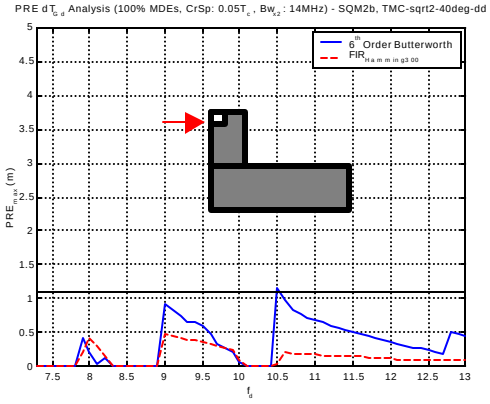

Figure 28. DD correlator dT_{Gd}'s using SQM2b (14.0MHz, 0.05T_c chip spacing; 2 Monitor Receivers, 100% MDE's; 40° elev.)

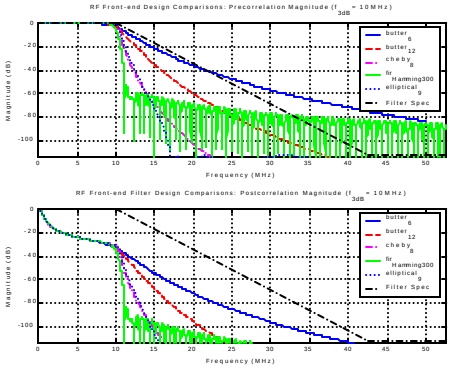

Figure 29. Various filter design implementations

Based on these analysis results, the ΔΔ Region 2 notch parameters were specified [8]. (See Figure 30 below.)

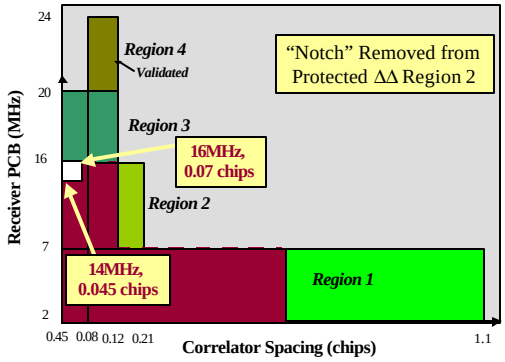

Figure 30. User design space and recommended "notch" parameters.

Magnitude Response Analysis

Figure 31 illustrates a suite of Butterworth filters (16 MHz PCB) used in the differential group delay analysis. Note that technically, only the (postcorrelation) 6th-order Butterworth filters completely met the LAAS specification. However, for (single-sided) frequencies higher than approximately 13MHz, the 60-150ns filters have magnitudes less than or equal to that of the 6th-order Butterworth. It follows that for Threat Model C, the critical threat model under consideration, all the filters except the 30ns design were *virtually* compliant with the LAAS interference requirement, since no frequencies above 13MHz excited the system. Also note that Threat Model B has frequencies as high as 17MHz. Had it been necessary to evaluate SQM2b using TM B for group delay sensitivity, few if any of these filter designs would have been acceptable.

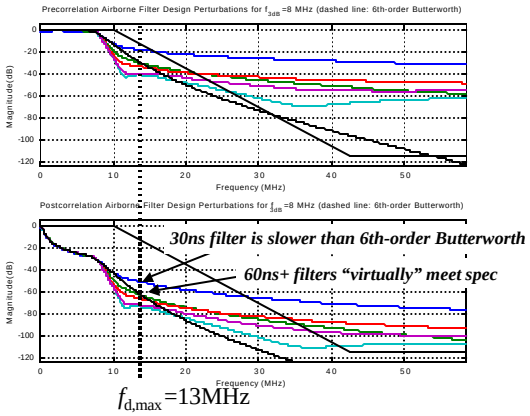

Figure 31. User filter perturbations (PCB=16MHz) compared to LAAS interference requirement.

As shown in the group delay for the ΔΔ Region 2 notch analysis, IIR filters with small passband dT_{Gd}'s tend to have extremely wide transition bandwidths. The unacceptable (30ns dT_{Gd}) filter from that analysis, however, violated the LAAS interference requirement. Still, such wide transition bandwidths have been found to result in unacceptably large PRE's for the very narrow ΔΔ receiver configurations.

Methodology

For this analysis, 4 interference-compliant, low-dT_{Gd} (3rd, 4th, 5th, and 6th-order) Butterworth filters were analyzed. As in the previous dT_{Gd} analyses, the ground monitor filter was FIR (zero dT_{Gd}). The resulting PRE contours are plotted *only for the receiver bandwidths where the filters meet the interference requirement*. The magnitude and dT_{Gd} responses of these filters are show in Figure 31. (Note that the maximum dT_{Gd}'s for all four filters are approximately 35ns.) In subsequent plots, Threat Model C PRE contours corresponding to a conservative elevation angle (30°) are provided. Though the E-L correlators were examined as well, only the ΔΔ contour plots (for the 100% MDE cases) are shown here [8]. (See Figures 32-36.) On each plot, the thick, shaded contours indicate the corresponding MERR threshold.

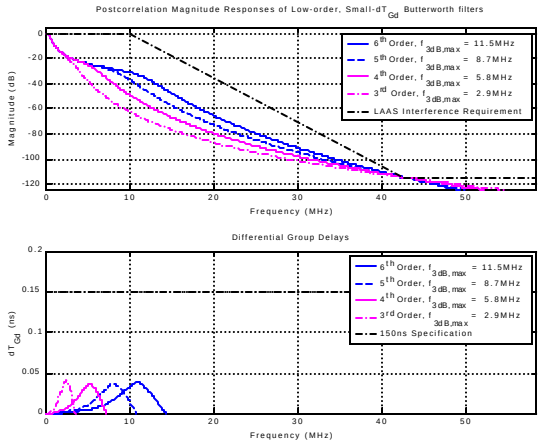

Figure 32. Maximum transition bandwidth filters.

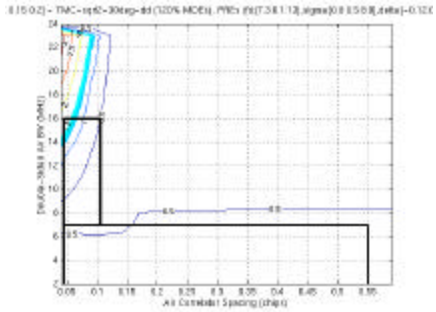

Figure 33. DD – TM C – 2 Monitor Receivers (100%MDE's) – 30° elev. – 6th-order Butterworth

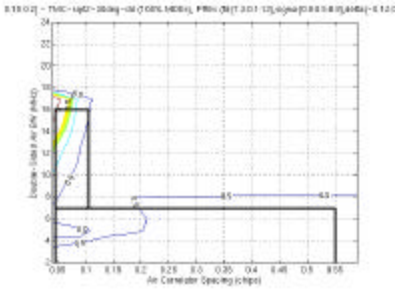

Figure 34. DD – TM C – 2 Monitor Receivers (100%MDE's) – 30° elev. – 5th-order Butterworth

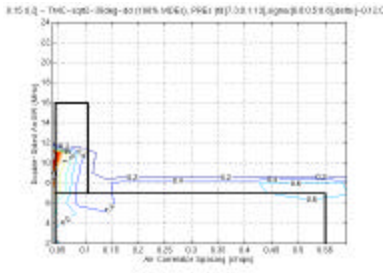

Figure 35. DD – TM C – 2 Monitor Receivers (100%MDE's) – 30° elev. – 4th-order Butterworth

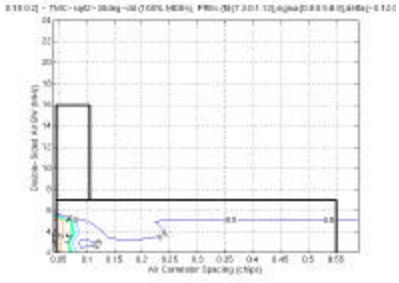

Figure 36. DD – TM C – 2 Monitor Receivers (100%MDE's) – 30° elev. – 3rd-order Butterworth

These analysis results indicate the need to specify a maximum transition bandwidth for the airborne user filters in addition *to the notch requirement* in order to protect both the ΔΔ regions. The maximum transition bandwidth should be upper-bounded by that of the 6th-order Butterworth. (See Figure 37.)

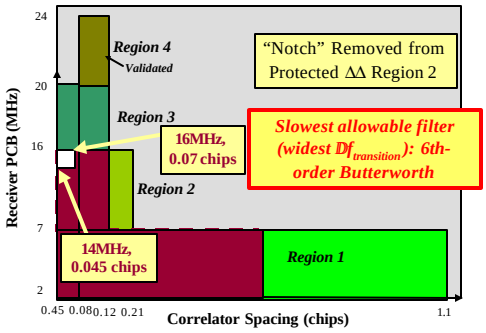

Figure 37. User design space with recommended "notch" and transition bandwidth parameters.

CONCLUSIONS

To design and evaluate a robust signal quality monitor, three analyses were performed. First, the maximum PRE's were compared to the respective MERR's for all elevation angles. Second, by perturbing only the filer group delays, the variation of those PRE's to filter differential group delay was investigated. Finally, by parameterizing the user filter transition bandwidth, the sensitivity of the PRE's to filter magnitude response variations was examined.

For SQM2b, this design methodology resulted in the following conclusions and recommendations:

- E-L correlators were protected against EWF's for all elevation angles and group delay variations (0-150ns) for 120% MDE's.
- ΔΔ correlators required a notch in Region 2 to meet MERR's at elevation angles >25° even for 100% MDE's.
- Recommendations (for ΔΔ compliance):
  - ΔΔ Region 2 Notch Parameters: 0.07Tc, 14MHz (lower-right corner)
  - Maximum Transition Bandwidth: 6th-order Butterworth

REFERENCES

[1] Enge, P. K., Phelts, R. E., Mitelman, A. M., "Detecting Anomalous signals from GPS Satellites," ICAO, GNSS/P, Toulouse, France, 1999.

[2] Akos, D. M., Phelts, R. E., Mitelman, A., Pullen S. Enge, P., "GPS-SPS Signal Quality Monitoring (SQM)," *Position Location and Navigation Symposium*, Conference Proceedings Addendum, IEEE PLANS, 2000.

[3] Shively, C., Brenner, M., Kline, P., "Multiple Ground Tests Protecting Against Satellite Correlation Symmetry Faults in LAAS (Revision 3), RTCA SC-159, 1999.

[4] *Specification: Performance Type One Local Area Augmentation System Ground Facility*. U.S. Federal Aviation Administration, Washington, D.C., FAA-E-2937, Sept., 21, 1999.

[5] Akos, D. M., Phelts, R. E., Pullen, S., Enge, P., "Signal Quality Monitoring: Test Results," *Proceedings of the 2000 National Technical Meeting*, Institute of Navigation, San Diego, CA, pp. 536-41, January 2000.

[6] Macabiau, C., Chatre, E., "Impact of Evil Waveforms on GBAS Performance," *Position Location and Navigation Symposium*, IEEE PLANS, pp. 22-9, 2000.

[7] Van Dierendonck, A. J., Akos, D., Pullen, S., Phelts, R. E. Enge, P., "Practical Implementation Considerations in the Detection of GPS Satellite Signal Failure," *Proceedings of the 2000 National Technical Meeting*, Institute of Navigation, June 2000.

[8] Phelts, R. E., Akos, D., Enge, P., "Signal Quality Monitoring Validation," ICAO, GNSSP WG-B, WP/29, Seattle, WA, 2000.